Barrier Lyapunov Function-Based Adaptive Fuzzy Attitude Tracking Control for Rigid Satellite with Input Delay and Output Constraint

Zepeng Zhou[a], Fanglai Zhu[a,*], Boli Chen[b] and Dezhi Xu[c]

[a]*College of Electronics and Information Engineering, Tongji University, Shanghai 201804, China*
[b]*Department of Electronic and Electrical Engineering, University College London, London WC1E 6BT, U.K.*
[c]*School of Internet of Things Engineering, Jiangnan University, Wuxi, 214122, China*

ARTICLE INFO

ABSTRACT

This paper investigates the adaptive attitude tracking problem for the rigid satellite involving output constraint, input saturation, input time delay, and external disturbance by integrating barrier Lyapunov function (BLF) and prescribed performance control (PPC). In contrast to the existing approaches, the input delay is addressed by Pade approximation, and the actual control input concerning saturation is obtained by utilizing an auxiliary variable that simplifies the controller design with respect to mean value methods or Nussbaum function-based strategies. Due to the implementation of the BLF control, together with an interval notion-based PPC strategy, not only the system output but also the transformed error produced by PPC are constrained. An adaptive fuzzy controller is then constructed and the predesigned constraints for system output and the transformed error will not be violated. In addition, a smooth switch term is imported into the controller such that the finite time convergence for all error variables is guaranteed for a certain case while the singularity problem is avoided. Finally, simulations are provided to show the effectiveness and potential of the proposed new design techniques.

1. Introduction

Due to the complicated deep space environment, the accurate attitude manipulation problem for the on-orbit spacecraft becomes challenging[1, 2]. During the past decade, many significant results have been reported for addressing the attitude tracking problem. These existing strategies usually include but not limited to the adaptive control[3, 4], finite/fixed time control[5, 6], sliding mode control[7], and fuzzy control[8].

According to the demands on the swiftness of the attitude tracking performance, the finite time control approaches have been investigated widely among many researchers. In [9], the researchers proposed a fractional order-based error compensation technique and all signals are guaranteed to be finite time stable. Moreover, by noting the finite convergence property, the fractional order-based error compensation in [9] is even applied to a quadrotor system with the prescribed output performance in [10]. In [11], the finite time tracking problem, integrating the state time-delay and event-triggered mechanism, is addressed on the basis of a proper Lyapunov-Krasovskii candidate function. In order to eliminate the influence caused by actuator failures, Cui et al.[12] proposed a command filter-based adaptive finite time control approach such that all the tracking errors can converge to the neighborhood of the origin within a finite time. On the basis of a novel BLF with adjustable parameters, the adaptive finite time controller design in [13] considered the facts of both the tracking errors' convergence time and the boundary constraint for the tracking errors. By means of adaptive fuzzy estimation method and BLF approach, the finite time convergence of the tracking error is guaranteed with respect to the implementation of the nonlinear switch term and the performance constraints are taken into account in [14]. Although these aforementioned strategies can provide finite time responses for the tracking errors, the singularity problem inherits from the fractional term used to achieve the finite time property has not been properly solved yet. In addition to the singularity problem caused by the fractional term, [15] even points out that the fast convergence rate for the tracking error cannot be guaranteed all the way by only utilizing the fractional order term, especially when the state is far way from the equilibrium. As a result, these problems will be discussed in this paper during the finite time controller design process.

---

*Corresponding author

✉ zhufanglai@tongji.edu.cn (F. Zhu)

In addition to the demand for the swift response, the problem of the amplitude constraint of the output error system has been studied intensively as well. The widely applied strategies involve the BLF method and the PPC control framework[16–18]. By integrating the adaptive fuzzy logic system, the output constraint problem with input delay is addressed on the basis of the BLF method in [19]. Similarly, Li et al. proposed a neural network-based output constraint controller in [20] and the full state constraint is hence guaranteed by the barrier Lyapunov function. In [21], the adaptive fault tolerant controller is presented on the framework of the PPC approach and the input saturation problem is handled with the Nussbaum gain method. To achieve the prescribed output tracking performance, the predesigned constraint is equivalently substituted by the state-constraint dynamics on the basis of the PPC method in [22] while the controller is constructed with the backstepping algorithm. It should be noted that these output constraint approaches are mainly developed on the backstepping control frameworks. However, the constraint for the transformed error given by the PPC strategy is not considered for most of the existing PPC approaches. This may lead to the large output of the virtual controller in order to stabilize the transformed error. In addition, one prominent drawback of the backstepping control is the differential explosion problem. To solve this, some attempts concerning output constraint and differential explosion problem can be found in [23, 24] with the utilization of command filter. Nevertheless, the constraint variables in [23, 24] are mixed up with the filter error such that the output constraint cannot be specified directly. Therefore, it remains a large space for researchers to develop a command filter-based controller that can constrain not only the output performance but also the transformed error provided the PPC method directly.

Although the output constraint control techniques have been intensively studied, the input saturation and input delay are rarely discussed simultaneously when there exists the output performance constraint. The widely used solutions for input saturation are mainly like mean value method and Nussbaum function. In [25], the asymmetric output saturation constraint is considered and the proposed mean value-based controller can provide a smooth control input. The Nussbaum function is used in [26] such that the impact caused by actuator saturation is compensated. By integrating Nussbaum function along with an auxiliary filter system, the smooth approximation of the input saturation is hence realized in [27]. Contrary to the mean value method as well as the Nussbaum function approach, an auxiliary variable-based input saturation solution is proposed in [28] and the controller design with respect to input saturation is simplified. However, the discussions about the input delay problem are missing from these above references. To address input saturation and input delay, some trials can be found in [29, 30]. By importing an auxiliary variable, the given state feedback controller in [30] can compensate the input delay and saturation in a sense of semi-global stability. Nonetheless, all these attempts only consider the linear systems. The correlated researches concerning input saturation and input delay for the nonlinear systems remain few, let alone the output constraint.

Motivated by the above discussions, the BLF-based control scheme proposed in the present paper will focus on the solution to the constraints of the attitude tracking error and the corresponding transformed error produced by the PPC strategy under the impact of input saturation and input delay. Firstly, the input delay is handled with the Pade approximation method, and by introducing an auxiliary dynamic system, the input saturation can then be approximated smoothly. To restrain the attitude tracking error, a novel interval notion-based PPC strategy is proposed. As for the constraint of the transformed error, the BLF method is applied during the construction of the controller. In addition, the command filter and the fuzzy logic system are introduced into controller design such that the controller has advantages on solving the differential explosion problem and producing the estimation of the unknown nonlinear term in the system, respectively. Compared to the existing researches, the main contributions are summarized as follows:

- Based on the Pade approximation method, the input delay is handled by introducing an intermediate variable $\chi(t)$. Meanwhile, differing from the existing mean value approach and Nussbaum function, the input saturation is addressed on the basis of the given auxiliary dynamic system, which not only simplify the controller design but also relax the demand on the pre-knowledge of the controller's initial value.

- Contrary to the existing PPC or BLF strategies, the constraints for both the attitude tracking error and the transformed error generated by the PPC are considered in the controller design and this control objective is realized by integrating the interval notion-based PPC approach and the BLF method. In addition, the singularity problem in traditional PPC method is avoided with the interval notion-based error transformation.

- To calculate the derivative of the virtual controller, the command filter is used. Differing from [23, 24], the variable of the BLF is only the transformed error. This provides a more direct aspect to investigate the parameter constraint problem when using command filter technique. The stability of the integrated control scheme is proved by invoking Lyapunov stability analysis. In addition, the control input is guaranteed to be continuous

even though there exists saturation and time delay.

The rest of this paper is organized as follows. Some preliminaries including the system dynamics and Pade approximation are given in Section 2. In Section 3, the interval notion-based error transformation is provided. Section 4 mainly discusses the adaptive fuzzy control strategy design. The simulation results are illustrated in Section 5 and Section 6 is the conclusion of this research.

2. Problem Formulation and Preliminaries

2.1. System Dynamics

On the basis of the modified Rodrigues parameters(MRPs), the rigid satellite attitude system is presented as [31],

$$\dot{\sigma} = \frac{1}{4}\left[\left(1 - \sigma^T\sigma\right)I_3 + 2\sigma^\times + 2\sigma\sigma^T\right]\omega = G(\sigma)\omega \tag{1}$$

$$J\dot{\omega} = -\omega^\times J\omega + Du(\nu(t - \tau)) + T_d \tag{2}$$

where $\sigma = [\sigma_1; \sigma_2; \sigma_3]$ and $\omega = [\omega_1; \omega_2; \omega_3]$ indicate the system's attitude and the angular velocity in body frame to the inertial frame respectively. $D \in \mathcal{R}^{3\times n}$ denotes the distribution matrix for n reaction wheels. $u(\cdot)$ represents the constrained control input with respect to physical saturation and $\nu \in \mathcal{R}^n$ is the ideal saturation-free control torque. τ is the fixed time delay. J represents the inertia matrix while $I_3 \in \mathcal{R}^{3\times3}$ is an identity matrix, $\sigma^\times, \omega^\times \in \mathcal{R}^{3\times3}$ are skew-symmetric matrices which satisfy $\mathcal{X}^\times = [0, -\mathcal{X}_3, \mathcal{X}_2; \mathcal{X}_3, 0, -\mathcal{X}_1; -\mathcal{X}_2, \mathcal{X}_1, 0]$ with $\mathcal{X} = [\mathcal{X}_1; \mathcal{X}_2; \mathcal{X}_3]$. The external disturbance T_d is denoted as $T_d = [T_{d1}; T_{d2}; T_{d3}]$. Additionally, for the case $\sigma^T\sigma > 1$, the MRPs are mapped to their shadow counterparts σ^s by $\sigma^s = \sigma/(\sigma^T\sigma)$. As a result, the MRPs indicate the shortest rotation distance to the origin and they are always bounded by a unit sphere. To achieve the expected attitude output performance, two error variables are given as,

$$\tilde{\sigma} = \sigma - \sigma_d, \quad \tilde{\omega} = \omega - \omega_d$$

where σ_d is the attitude reference signal and ω_d is the desired angular velocity which is also known as the virtual controller under the framework of backstepping control.

2.2. Fuzzy Logic System(FLS)

It has been proven that any nonlinear function $F(x)$ can be approximated via FLS with IF-THEN rules:

R^m:If x_1 is X_1^m and x_2 is X_2^m, ..., x_n is X_n^m,
　　Then y is Y^m, $m = 1, 2, \ldots, q$

where $x = [x_1; \ldots; x_n]$ and y are the input and output of the FLS. The fuzzy sets X_i^m and Y^m are related to the fuzzy function $\mu_{X_i^m}(x_i)$ and $\mu_{Y^m}(y)$. q represents the amount of the fuzzy rules. According to singleton function, center average defuzzification and product inference, $y(x)$ can be written as [32],

$$y(x) = \frac{\Sigma_{m=1}^q \bar{y}_m \Pi_{i=1}^n \mu_{X_i^m}(x_i)}{\Sigma_{m=1}^q (\Pi_{i=1}^n \mu_{X_i^m}(x_i))}$$

where $\bar{y}_m = \max_{y\in\mathcal{R}} \mu_{Y^m}(y)$. Defining $\Lambda_m = \frac{\Pi_{i=1}^n \mu_{X_i^m}(x_i)}{\Sigma_{m=1}^q (\Pi_{i=1}^n \mu_{X_i^m}(x_i))}$ as the fuzzy basis function and $\varkappa = [\bar{y}_1; \ldots; \bar{y}_q]$ and $\Lambda(x) = [\Lambda_1; \ldots; \Lambda_q]$, then the output of the FLS is given as $y(x) = \varkappa^T\Lambda$.

Lemma 1 ([33]). Consider a smooth function $F(x)$ defined on a compact set Ω, for any given constant $\hbar$, there exists a FLS output $\varkappa^T\Lambda(x)$ such that $\sup_{x\in\Omega} |F(x) - \varkappa^T\Lambda(x)| \leq \hbar$ always holds.

2.3. Control Input with Saturation and Time Delay

In order to eliminate the impact caused by input delay τ, the Pade approximation method based on the Laplace space is constructed. By transforming $u(v(t - \tau))$ into Laplace space, it has,

$$\mathcal{L}[u(v(t - \tau))] = \exp(-\tau s)\mathcal{L}[u(v(t))]$$
$$\approx (1 - \tau s/2)/(1 + \tau s/2) \cdot \mathcal{L}[u(v(t))]$$

where s is the Laplace operator and $\mathcal{L}[u(v(t - \tau))]$ is the transformation of $u(v(t - \tau))$ with respect to Laplace space. In addition, a virtual internal variable $\chi(t)$ is imported here and it satisfies,

$$(1 - \tau s/2)/(1 + \tau s/2)\mathcal{L}[u(v(t))] = \mathcal{L}[\chi(t)] - \mathcal{L}[u(v(t))] \tag{3}$$

Furthermore, (3) can be rewritten as,

$$2\mathcal{L}[u(v(t))] = \mathcal{L}[\chi(t)] + 1/2 \cdot \tau s\mathcal{L}[\chi(t)] \tag{4}$$

Taking the inverse Laplace transformation for (4) gives,

$$\dot{\chi}(t) = 2\lambda u(v(t)) - \lambda \chi(t) \tag{5}$$

where $\lambda = 2/\tau$. Then, (2) is modified as,

$$\dot{\omega} = -J^{-1}\omega^{\times}J\omega + J^{-1}D\chi(t) - J^{-1}Du(v(t)) + J^{-1}T_d \tag{6}$$

For the input saturation problem, the constrained input $u(v(t))$ is defined as,

$$u_i(v_i(t)) = \begin{cases} v_i, & |v_i| < u_{\max} \\ u_{\max}\text{sign}(v_i), & |v_i| \geq u_{\max} \end{cases}$$

where $u_{\max}$ is the maximum control power for each channel. $u_i(\cdot)$ and $v_i(t)$ are the ith constrained and constrained-free control input in $u(v(t))$. As is shown in [21], the following $\tanh(\cdot)$ function can be used to approximate $u(v(t))$,

$$g(v_i) = u_{\max} \cdot \tanh(v_i(t)/u_{\max})$$
$$= u_{\max} \cdot \frac{\exp(v_i(t)/u_{\max}) - \exp(-v_i(t)/u_{\max})}{\exp(v_i(t)/u_{\max}) + \exp(-v_i(t)/u_{\max})} \tag{7}$$

According to (7), $u(v(t))$ can be replaced by,

$$u(v(t)) = g(v(t)) + e_s(v(t))$$
$$= u_{\max} \cdot \tanh(v(t)/u_{\max}) + e_s(v(t)) \tag{8}$$

where $g(v(t)) = [g(v_1); \ldots; g(v_n)]$ and $e_s(v(t)) = u(v(t)) - g(v(t))$ is the approximation error. From [21], e_s is bounded and satisfies $|e_{si}| = |u_i(v_i) - g(v_i)| \leq u_{max}(1 - \tanh(1))$. In order to design the control input $v(t)$, an auxiliary variable ζ is given as,

$$\dot{\zeta} = -\zeta + (g(v) - v) \tag{9}$$

Therefore, according to (5)-(9), the whole system is represented as,

$$\dot{\sigma} = G(\sigma)\omega \tag{10}$$
$$\dot{\omega} = -J^{-1}\omega^{\times}J\omega + J^{-1}D\chi - J^{-1}Dg(v) - J^{-1}De_s(v) + J^{-1}T_d \tag{11}$$
$$\dot{\chi} = -\lambda\chi + 2\lambda g(v) + 2\lambda e_s(v) \tag{12}$$

Remark 1. To transform the constrained input $g(v(t))$ into a constrained-free one $v(t)$ in controller design process, two main strategies have been proposed, namely mean value approach[21, 25] and Nussbaum function method[26, 28]. In this paper, an auxiliary variable ζ is imported. Differing from the previous methods, it brings two main advantages. One is that it does not need the hypothesis in mean value approach that $v(0) = 0$. The other is that it provides a simplifed way to develop the controller when compared to the Nussbaum function-based method. These merits are also revealed in the controller design.

Remark 2. Differing from many existing results, such as the one in [34], the input delay τ is addressed by Pade approximation and the complex deduction process caused by Lyapunov-Krasovskii function in [34] is avoided in the present paper. Moreover, by referring [35], not only the constant time delay but also the time-varying delay can be addressed by importing Pade approximation. In addition, according to (6), the controller design coupling problem for simultaneously addressing input delay and saturation is solved. Therefore, in view of dealing with time-delay, this paper can be viewed as an extension of [34].

2.4. Problem Formulation

The objectives of the control approach in this paper are,

- Constructing a novel BLF-based PPC strategy so as to guarantee the predesigned output performances while the stability for the whole system is also ensured.

- The input saturation and the input delay problems should be addressed subject to the control strategy design.

The structure of the proposed control approach is illustrated in Fig. 1. From Fig. 1, the constraints for $\tilde{\sigma}$ and the transformed error $\varepsilon(t)$ are guaranteed by the PPC and BLF method separately. The command filter is used to estimate the virtual controller ω_d and its derivative during the controller design. In addition, a command filter is presented as[36],

$$\dot{\omega}_{ci} = -k_{\varpi 1}|\omega_{ci} - \omega_{di}|^{1/2}\text{sign}(\omega_{ci} - \omega_{di}) + \varpi_i$$
$$\dot{\varpi}_i = -k_{\varpi 2}\text{sign}(\varpi_i - \dot{\omega}_{ci})$$

where $k_{\varpi 1}$ and $k_{\varpi 2} > 0$, ω_{di} is the input signal which is the ith element in ω_d. ω_{ci} and $\dot{\omega}_{ci}$ are the estimations of ω_{di} and its derivative, respectively.
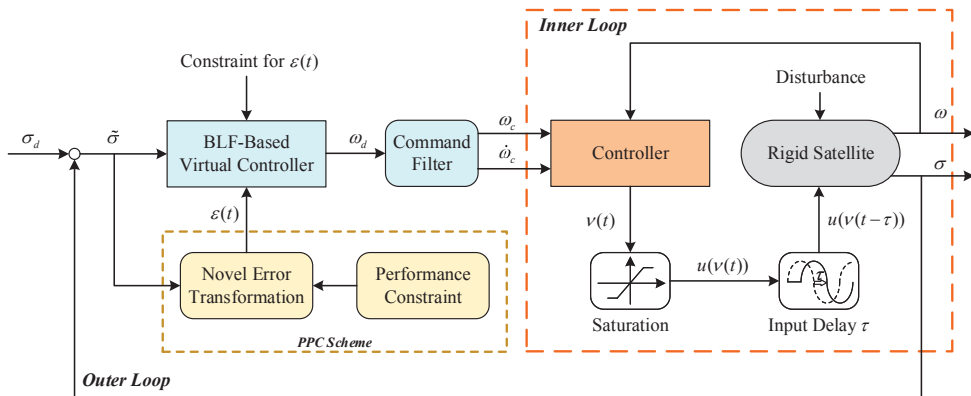

Figure 1: The structure of the control scheme

For the sake of further analysis, following lemmas and the assumption are needed.

Lemma 2 ([21]). For any $x \in \mathcal{R}$ and $y \in \mathcal{R}^+$, if $|x| < y$, then it holds that $\log[y^2/(y^2 - x^2)] \leq x^2/(y^2 - x^2)$.

Lemma 3 ([27]). For any $x \in \mathcal{R}$ and $z \in \mathcal{R}^+$, it satisfies that $0 \leq |x| - x\tanh(x/z) \leq k_z z$ where $k_z \approx 0.2785$.

Lemma 4 ([37]). For any $0 < \gamma_0 < 1$, a, $b > 0$, if the Lyapunov function $V(x)$ satisfies $\dot{V}(x) + aV(x) + bV^{\gamma_0}(x) \leq 0$, then the Lyapunov function $V(x)$ approaches 0 within T_{reach} and the convergence time T_{reach} satisfies that $T_{reach} \leq 1/(a(1 - \gamma_0)) \log[(aV^{1-\gamma_0}(0) + b)/b]$.

Proposition 1 ([38, 39]). *For any $0 < \gamma_0 < 1$, a, $b > 0$, if the Lyapunov function $V(x)$ satisfies $\dot{V}(x) + aV(x) + bV^{\gamma_0}(x) \leq V_\Delta$ and $V_\Delta > 0$, then the state x in the Lyapunov function $V(x)$ approaches the neighborhood of the origin while the solution set $\mathcal{S}$ satisfies $\mathcal{S} = \left\{ x | V(x) \leq \frac{V_\Delta}{(1-c)a} \right\}$ and the convergence time T_{reach} holds $T_{reach} \leq 1/(ca(1 - \gamma_0)) \log[(caV^{1-\gamma_0}(0) + b)/b]$ where $0 < c < 1$.*

Proof: Considering the following inequality,

$$\dot{V}(x) + acV(x) + bV^{\gamma_0}(x) + (1 - c)aV(x) \leq V_\Delta \tag{13}$$

For the case when $V(x) > V_\Delta / [(1 - c)a]$, (13) becomes $\dot{V}(x) + acV(x) + bV^{\gamma_0}(x) \leq 0$. Therefore, according to Lemma 4, the solution for x converges to the set $\mathcal{S} = \left\{ x | V(x) \leq \frac{V_\Delta}{(1-c)a} \right\}$ within a finite time satisfying $T_{reach} \leq 1/(ca(1 - \gamma_0)) \log[(caV^{1-\gamma_0}(0) + b)/b]$. According to the previous deduction, the trajectory for x will not exceed set $\mathcal{S}$ for the case when $V(x) \leq V_\Delta / [(1 - c)a]$. $\square$

Lemma 5 ([40]). For $0 < \gamma_0 < 1$ and $x_i \in \mathcal{R}$, $i = 1, \ldots, n$, then it holds that $\sum_{i=1}^{n} |x_i|^{\gamma_0+1} \geq (\sum_{i=1}^{n} |x_i|^2)^{(\gamma_0+1)/2}$.

Assumption 1. The external disturbance T_d is bounded.

3. Novel Error Transformation

To perform tracking error transformation, a finite-time decreasing function $\rho(t)$ is defined,

$$\rho = \begin{cases} (\rho_0 - \rho_{t_f})\exp(lt/(t - t_f)) + \rho_{t_f}, & 0 \leq t < t_f \\ \rho_{t_f}, & t \geq t_f \end{cases} \tag{14}$$

where l is the decreasing index, ρ_0 and ρ_{t_f} satisfy $\rho_0 = \lim_{t \to 0} \rho(t)$ and $\rho_{t_f} = \lim_{t \to t_f} \rho(t)$. t_f is the reaching time. To restrain the time response of the attitude tracking error $\tilde{\sigma}$, the output constraint is given as,

$$-\underline{\mu}_i(t)\underline{\rho}_i(t) < \tilde{\sigma}_i < \overline{\mu}_i(t)\overline{\rho}_i(t), \quad i = 1, 2, 3 \tag{15}$$

where $\overline{\rho}_i(t)$ and $\underline{\rho}_i(t)$ can be inferred from (14) while $\overline{\mu}_i(t)$ and $\underline{\mu}_i(t)$ hold,

$$\underline{\mu}_i(t) = \mathcal{G}_{i1}/(\mathcal{G}_{i2} - \mathcal{G}_{i2}\exp(-\varsigma_{i1}t) + \mathcal{G}_{i3})$$
$$\overline{\mu}_i(t) = \mathcal{G}_{i4}/(\mathcal{G}_{i5} - \mathcal{G}_{i5}\exp(-\varsigma_{i2}t) + \mathcal{G}_{i6})$$

where $\varsigma_{i1,i2} > 0$. $\mathcal{G}_{ij} > 0$, $i = 1, 2, 3$, $j = 1, \ldots, 6$ and $\mathcal{G}_{i1} > \mathcal{G}_{i3} > 0$, $\mathcal{G}_{i4} > \mathcal{G}_{i6} > 0$. It can be easily shown that $\overline{\mu}_i(t)$ and $\underline{\mu}_i(t)$ in (15) satisfy [41],

1) $\underline{\mu}_i(t), \overline{\mu}_i(t) > 0$ and $\dot{\underline{\mu}}_i(t), \dot{\overline{\mu}}_i(t) < 0$,

2) $\underline{\mu}_i(0) > C_1$ and $\lim_{t \to \infty} \underline{\mu}_i(t) = C_1$, $C_1 \in \mathcal{R}^+$,

3) $\overline{\mu}_i(0) > C_2$ and $\lim_{t \to \infty} \overline{\mu}_i(t) = C_2$, $C_2 \in \mathcal{R}^+$.

For any given interval, the variable in this interval can be presented by the interval's upper and lower boundaries. According to (15), it evidently indicates that there exists ψ_i satisfying $0 < \psi_i < 1$ such that,

$$\tilde{\sigma}_i = \psi_i \overline{\mu}_i \overline{\rho}_i - (1 - \psi_i)\underline{\mu}_i \underline{\rho}_i \tag{16}$$

Remark 3. To verify (16), a function $\alpha(\psi_i)$ is defined as $\alpha(\psi_i) = (\bar{\mu}_i\bar{\rho}_i + \underline{\mu}_i\underline{\rho}_i)\psi_i - \underline{\mu}_i\underline{\rho}_i$. The derivation for $\alpha(\psi_i)$ holds $\dot{\alpha}(\psi_i) = \bar{\mu}_i\bar{\rho}_i + \underline{\mu}_i\underline{\rho}_i$. Due to $\bar{\mu}_i\bar{\rho}_i + \underline{\mu}_i\underline{\rho}_i > 0$, $\alpha(\psi_i)$ is a strictly increasing function for $\psi_i \in (0, 1)$. Therefore, $\alpha(\psi_i) \in (-\underline{\mu}_i\underline{\rho}_i, \bar{\mu}_i\bar{\rho}_i)$ and the interval notion-based expression (16) is valid.

Therefore, it can obtain that,

$$\psi_i = \frac{\tilde{\sigma}_i + \underline{\mu}_i\underline{\rho}_i}{\bar{\mu}_i\bar{\rho}_i + \underline{\mu}_i\underline{\rho}_i} \tag{17}$$

while the desired unconstraint transformation variable ψ_{id} is given as,

$$\psi_{id} = \frac{\underline{\mu}_i\underline{\rho}_i}{\bar{\mu}_i\bar{\rho}_i + \underline{\mu}_i\underline{\rho}_i} \tag{18}$$

By referring (17) and (18), the transformation error ε_i is defined as,

$$\varepsilon_i = \psi_i - \psi_{id} = \frac{\tilde{\sigma}_i}{\bar{\mu}_i\bar{\rho}_i + \underline{\mu}_i\underline{\rho}_i} \tag{19}$$

From (19), it is obvious that $\varepsilon_i \in (-1, 1)$. Taking the time derivative for ε_i gives,

$$\dot{\varepsilon}_i = \frac{\dot{\tilde{\sigma}}_i \cdot \left(\bar{\mu}_i\bar{\rho}_i + \underline{\mu}_i\underline{\rho}_i\right) - \tilde{\sigma}_i \cdot \left(\dot{\bar{\mu}}_i\bar{\rho}_i + \bar{\mu}_i\dot{\bar{\rho}}_i + \dot{\underline{\mu}}_i\underline{\rho}_i + \underline{\mu}_i\dot{\underline{\rho}}_i\right)}{\left(\bar{\mu}_i\bar{\rho}_i + \underline{\mu}_i\underline{\rho}_i\right)^2}$$

$$= \Phi_i\dot{\tilde{\sigma}}_i + \Psi_i \tag{20}$$

where Φ_i and Ψ_i are defined as,

$$\Phi_i = \left(\bar{\mu}_i\bar{\rho}_i + \underline{\mu}_i\underline{\rho}_i\right) / \left(\bar{\mu}_i\bar{\rho}_i + \underline{\mu}_i\underline{\rho}_i\right)^2$$

$$\Psi_i = -\tilde{\sigma}_i \cdot \left(\dot{\bar{\mu}}_i\bar{\rho}_i + \bar{\mu}_i\dot{\bar{\rho}}_i + \dot{\underline{\mu}}_i\underline{\rho}_i + \underline{\mu}_i\dot{\underline{\rho}}_i\right) / \left(\bar{\mu}_i\bar{\rho}_i + \underline{\mu}_i\underline{\rho}_i\right)^2$$

Consequently, from (20), it is immediate to obtain,

$$\dot{\varepsilon} = \Phi G(\sigma)\omega + \Psi - \Phi\dot{\sigma}_d \tag{21}$$

where $\varepsilon = [\varepsilon_1, \varepsilon_2, \varepsilon_3]^T$ and $\Phi = \text{diag}\{\Phi_1, \Phi_2, \Phi_3\}$, $\Psi = [\Psi_1, \Psi_2, \Psi_3]^T$.

Remark 4. This interval notion-based PPC strategy is truly an original one and it provides a more clear and simpler way to depict the relationship between the output constraints and the attitude tracking errors. In addition, the interval notion-based expression (16) is based on the basic algebraic calculation while the tanh-liked transformation is necessary in [41]. As a result, the proposed error transformation method can lower the complexity of the PPC structure.

Remark 5. From the computation burden aspect, this approach can be dramatically simplified when confronted with symmetric performance boundary constraints and the transformation error ε_i in (19) can be rewritten as $\varepsilon_i = \tilde{\sigma}_i / (2\bar{\mu}_i\bar{\rho}_i)$. This leads to a simple dynamic representation for ε because the computation burden is alleviated. However, the inverse operation of the tanh-liked function in [41] is necessary to separate the transformation error. Therefore, the construction for the transformation error is more direct and simpler than the traditional methods in [21, 41] under this circumstance.

Remark 6. According to (15), the variables $\underline{\mu}_i(t)$ and $\bar{\mu}_i(t)$ are able to enlarge the distance between the tracking error $\tilde{\sigma}$ and the boundary $-\underline{\mu}_i(t)\underline{\rho}_i(t)$ or $\overline{\mu}_i(t)\overline{\rho}_i(t)$ by adopting $\mathcal{G}_{i1} \geq \mathcal{G}_{i2} + \mathcal{G}_{i3}$ and $\mathcal{G}_{i4} \geq \mathcal{G}_{i5} + \mathcal{G}_{i6}$. This results in a smaller control power demand for stabilizing ε_i at the initial phase. In addition, (15) also indicates that the decreasing ratio of the performance boundary is affected by of $-\underline{\mu}_i(t)\underline{\rho}_i(t)$ or $\overline{\mu}_i(t)\overline{\rho}_i(t)$. Therefore, to maintain a moderate control torque during the attitude manipulation, the decreasing rate indices ς_{i1} and ς_{i2} for $\underline{\mu}_i(t)$ and $\bar{\mu}_i(t)$ are suggested to be small ones.

4. Barrier Lyapunov Function-Based PPC Controller

In this section, a novel BLF-based PPC controller will be constructed within the framework of backstepping method while the command filter and adaptive fuzzy approximation strategy are also utilized.

To construct the virtual controller, a log-type barrier Lyapunov function is introduced,

$$V_1 = \frac{1}{2} \sum_{i=1}^{3} \log \frac{k_b^2}{k_b^2 - \varepsilon_i^2} \tag{22}$$

where the barrier variable $k_b = 1$. Taking the time derivative of V_1 gives,

$$\dot{V}_1 = \sum_{i=1}^{3} \frac{\varepsilon_i \dot{\varepsilon}_i}{k_b^2 - \varepsilon_i^2} = \sum_{i=1}^{3} \frac{\varepsilon_i}{k_b^2 - \varepsilon_i^2} \left(\Phi_i \dot{\sigma}_i + \Psi_i - \Phi_i \dot{\sigma}_{di} \right) \tag{23}$$

To achieve a finite time convergence, a proper dynamic process for σ_i is assumed to be like,

$$\dot{\sigma}_i = \Phi_i^{-1} \left(-k_1 \varepsilon_i - \Psi_i + \Phi_i \dot{\sigma}_{di} - k_{\varphi 1} \varphi_{\varepsilon_i} \right) \tag{24}$$

where k_1 and $k_{\varphi 1}$ are positive scalars. The nonlinear term $\varphi_{\varepsilon i}(\varepsilon_i)$ in (24) is selected as,

$$\varphi_{\varepsilon_i}(\varepsilon_i) = \begin{cases} \varepsilon_i^\gamma \left(k_b^2 - \varepsilon_i^2 \right)^{\frac{1-\gamma}{2}}, & \text{if } |\varepsilon_i| \geq \Delta_1 \\ \theta_1 \varepsilon_i + \theta_2 \varepsilon_i^3, & \text{if } |\varepsilon_i| < \Delta_1 \end{cases}$$

where $0 < \gamma < 1$ and $\Delta_1 < k_b$ is a small positive constant. θ_1 and θ_2 are defined as,

$$\theta_1 = \left(\Delta_1 \text{sign}(\varepsilon_1) \right)^{\gamma - 1} \left(k_b^2 - \Delta_1^2 \right)^{\frac{1-\gamma}{2}} - \theta_2 \Delta_1^2$$

$$\theta_2 = \frac{\text{sign}(\varepsilon_i)}{2\Delta_1^3} (\gamma - 1) \left(\Delta_1 \text{sign}(\varepsilon_i) \right)^\gamma \left[\left(k_b^2 - \Delta_1^2 \right)^{\frac{1-\gamma}{2}} + \left(\Delta_1 \text{sign}(\varepsilon_1) \right)^2 \left(k_b^2 - \Delta_1^2 \right)^{-\frac{1+\gamma}{2}} \right]$$

Substituting (24) into (23) yields,

$$\dot{V}_1 = \sum_{i=1}^{3} \frac{\varepsilon_i}{k_b^2 - \varepsilon_i^2} \left(\Phi_i \dot{\sigma}_i + \Psi_i - \Phi_i \dot{\sigma}_{di} \right)$$

$$= -k_1 \sum_{i=1}^{3} \frac{\varepsilon_i^2}{k_b^2 - \varepsilon_i^2} - k_{\varphi 1} \sum_{i=1}^{3} \frac{\varepsilon_i}{k_b^2 - \varepsilon_i^2} \varphi_{\varepsilon_i} \tag{25}$$

1) For the case when $|\varepsilon_i| \geq \Delta_1$, $\dot{V}_1$ holds,

$$\dot{V}_1 = -k_1 \sum_{i=1}^{3} \frac{\varepsilon_i^2}{k_b^2 - \varepsilon_i^2} - k_{\varphi 1} \sum_{i=1}^{3} \frac{\varepsilon_i^{1+\gamma}}{k_b^2 - \varepsilon_i^2} \left(k_b^2 - \varepsilon_i^2 \right)^{\frac{1-\gamma}{2}}$$

$$\leq -k_1 \sum_{i=1}^{3} \log \frac{k_b^2}{k_b^2 - \varepsilon_i^2} - k_{\varphi 1} \sum_{i=1}^{3} \left(\log \frac{k_b^2}{k_b^2 - \varepsilon_i^2} \right)^{\frac{1+\gamma}{2}} \tag{26}$$

According to Lemma 2 and (25)-(26), we have,

$$\dot{V}_1 \leq -2k_1 V_1 - 2^{\frac{1+\gamma}{2}} k_{\varphi 1} V_1^{\frac{1+\gamma}{2}} \tag{27}$$

By retrospecting Lemma 4 and (27), the designed $\dot{\sigma}_i$ can guarantee the finite time convergent property of ε_i under this circumstance.

2) For the case when $|\varepsilon_i| < \Delta_1$, $\dot{V}_1$ satisfies,

$$
\begin{aligned}
\dot{V}_1 = &- k_1 \sum_{i=1}^{3} \frac{\varepsilon_i^2}{k_b^2 - \varepsilon_i^2} - k_{\varphi_1} \theta_1 \sum_{i=1}^{3} \frac{\varepsilon_i^2}{k_b^2 - \varepsilon_i^2} - k_{\varphi_1} \theta_2 \sum_{i=1}^{3} \frac{\varepsilon_i^4}{k_b^2 - \varepsilon_i^2} \\
\leq &- k_1 \sum_{i=1}^{3} \log \frac{k_b^2}{k_b^2 - \varepsilon_i^2} - k_{\varphi_1} \theta_1 \sum_{i=1}^{3} \log \frac{k_b^2}{k_b^2 - \varepsilon_i^2} \\
\leq &- 2(k_1 + k_{\varphi_1} \theta_1) V_1
\end{aligned}
\tag{28}
$$

Then it concludes that ε_i is asymptotically stable.

Due to the implement of backstepping control, it should be emphasized that the construction of (24) is based on the stability of the inner loop which means $\omega = \omega_{d0}$. However, the difference between ω and ω_{d0} cannot be neglected during the attitude manipulation process.

Therefore, $\dot{\sigma}$ can be represented as,

$$
\begin{aligned}
\dot{\sigma} =& \Phi^{-1} \left(-k_1 \varepsilon - \Psi - k_{\varphi_1} \varphi_\varepsilon \right) + \dot{\sigma}_d \\
=& G(\sigma)(\tilde{\omega} + \omega_d)
\end{aligned}
\tag{29}
$$

where $\varphi_\varepsilon = [\varphi_{\varepsilon 1}; \varphi_{\varepsilon 2}; \varphi_{\varepsilon 3}]$. Consequently, an ideal virtual controller ω_{d0} is chosen as,

$$
\omega_{d0} = G^{-1}(\sigma) \Phi^{-1} \left(-k_1 \varepsilon - \Psi - k_{\varphi_1} \varphi_\varepsilon + \Phi \dot{\sigma}_d \right)
\tag{30}
$$

By referring (29) and (30), (25) can be further rewritten as,

$$
\begin{aligned}
\dot{V}_1 =& \sum_{i=1}^{3} \frac{\varepsilon_i}{k_b^2 - \varepsilon_i^2} \left(\Phi_i \dot{\sigma}_i + \Psi_i - \Phi_i \dot{\sigma}_{di} \right) \\
=& - k_1 \sum_{i=1}^{3} \frac{\varepsilon_i^2}{k_b^2 - \varepsilon_i^2} - k_{\varphi_1} \sum_{i=1}^{3} \frac{\varepsilon_i}{k_b^2 - \varepsilon_i^2} \varphi_{\varepsilon_i} \\
&+ \varepsilon^T F(\varepsilon) \Phi G(\sigma) \tilde{\omega}
\end{aligned}
\tag{31}
$$

where $F(\varepsilon) = \text{diag}\{[1/(k_b^2 - \varepsilon_1^2); 1/(k_b^2 - \varepsilon_2^2); 1/(k_b^2 - \varepsilon_3^2)]\}$.

Due to the implement of the command filter, the difference ω_Δ between the filtered signal ω_c and ω_d is defined as $\omega_\Delta = \omega_c - \omega_d$. Then, (29) can be rewritten as,

$$
\dot{\sigma} = G(\sigma)(\bar{\omega} + \omega_d + \omega_\Delta)
\tag{32}
$$

where $\bar{\omega} = \omega - \omega_c$. According to (32), (31) is represented as,

$$
\begin{aligned}
\dot{V}_1 =& - k_1 \sum_{i=1}^{3} \frac{\varepsilon_i^2}{k_b^2 - \varepsilon_i^2} - k_{\varphi_1} \sum_{i=1}^{3} \frac{\varepsilon_i}{k_b^2 - \varepsilon_i^2} \varphi_{\varepsilon_i} \\
&+ \varepsilon^T F(\varepsilon) \Phi G \bar{\omega} + \varepsilon^T F(\varepsilon) \Phi G \omega_\Delta
\end{aligned}
\tag{33}
$$

Consequently, an adaptive fuzzy virtual controller is given as,

$$
\omega_d = G^{-1}(\sigma) \Phi^{-1} \left[-k_1 \varepsilon - \Psi - k_{\varphi_1} \varphi_\varepsilon - \frac{F(\varepsilon)}{2\epsilon} \varepsilon - \Phi \dot{\sigma}_d - \frac{\hat{\varrho} F(\varepsilon) \phi}{2\eta} \varepsilon \right]
\tag{34}
$$

$$
\dot{\hat{\varrho}} = \frac{\kappa_1 \sum_{i=1}^{3} \frac{\varepsilon_i^2}{(k_b^2 - \varepsilon_i^2)^2} \phi_i^T \phi_i}{2\eta} - k_\varrho \left(2\hat{\varrho} - \ell_\varrho \right)
\tag{35}
$$

where k_ϱ, η, ϵ, ℓ_ϱ, and κ_1 are positive scalars, $\phi = \text{diag}\{[\phi_1^T \phi_1; \phi_2^T \phi_2; \phi_3^T \phi_3]\}$. Defining $\varrho = \max\{\|\varrho_1\|^2, \|\varrho_2\|^2, \|\varrho_3\|^2\}$ and $\hat{\varrho}$ is the estimation of ϱ. The detailed definitions for ϕ_i, and ϱ_i, $i = 1, 2, 3$ will be given in later part.

For the inner loop, an auxiliary variable is constructed as,

$$\Upsilon = \bar{\omega} + \frac{J^{-1}D\chi}{\lambda} - J^{-1}D\zeta \tag{36}$$

Taking the time derivative for (36), it obtains,

$$
\begin{aligned}
\dot{\Upsilon} =& \dot{\omega} - \dot{\omega}_c - J^{-1}D\chi + 2J^{-1}Dg(v) + 2J^{-1}De_s(v) \\
&+ J^{-1}D\zeta - J^{-1}Dg(v) + J^{-1}Dv \\
=& -J^{-1}\omega^\times J\omega + J^{-1}D\chi - J^{-1}Dg(v) - J^{-1}De_s(v) \\
&- \dot{\omega}_c - J^{-1}D\chi + 2J^{-1}Dg(v) + 2J^{-1}De_s(v) \\
&+ J^{-1}D\zeta - J^{-1}Dg(v) + J^{-1}Dv + J^{-1}T_d \\
=& -J^{-1}\omega^\times J\omega + J^{-1}Dv + J^{-1}D\zeta \\
&+ J^{-1}(De_s(v) + T_d) - \dot{\omega}_c \tag{37}
\end{aligned}
$$

Then another Lyapunov function V_2 for the inner loop is chosen as,

$$V_2 = V_1 + \frac{1}{2}\Upsilon^T\Upsilon \tag{38}$$

Referring (37), the time derivative of (38) holds,

$$
\begin{aligned}
\dot{V}_2 =& -k_1 \sum_{i=1}^{3} \frac{\varepsilon_i^2}{k_b^2 - \varepsilon_i^2} - k_{\varphi 1} \sum_{i=1}^{3} \frac{\varepsilon_i}{k_b^2 - \varepsilon_i^2} \varphi_{\varepsilon_i} \\
&+ \varepsilon^T F(\varepsilon)\Phi G\bar{\omega} + \varepsilon^T F(\varepsilon)\Phi G\omega_\Delta \\
&+ \Upsilon^T \left[-J^{-1}\omega^\times J\omega + J^{-1}Dv + J^{-1}D\zeta + J^{-1}(De_s(v) + T_d) - \dot{\omega}_c \right]
\end{aligned}
$$

Then, the adaptive finite time controller $v(t)$ is designed as,

$$v = D^{-1}J\left(-k_2\Upsilon - k_{\varphi 2}\varphi_\Upsilon + \dot{\omega}_c + J^{-1}\omega^\times J\omega - \tanh(\Upsilon/z)\hat{\bar{E}}\right) - \zeta \tag{39}$$

$$\dot{\hat{\bar{E}}} = \kappa_2 \tanh(\Upsilon/z)\Upsilon - k_E\left(2\hat{\bar{E}} - \ell_E\right) \tag{40}$$

where k_2, κ_2, $k_{\varphi 2}$, and k_E are positive scalars. ℓ_E is a positive vector. $\hat{\bar{E}}$ is the estimation of $\bar{E}$ and the estimation error $\tilde{\bar{E}}$ is $\tilde{\bar{E}} = \bar{E} - \hat{\bar{E}}$. The definition for $\bar{E}$ will be given in later part. The nonlinear term $\varphi_\Upsilon(\Upsilon)$ is developed as,

$$
\varphi_{\Upsilon i}(\Upsilon_i) = \begin{cases} \Upsilon_i^\gamma, & \text{if } |\Upsilon_i| \geq \Delta_2 \\ \theta_3\Upsilon_i + \theta_4\Upsilon_i^3, & \text{if } |\Upsilon_i| < \Delta_2 \end{cases}
$$

where Δ_2 is a positive scalar. θ_3 and θ_4 are selected as,

$$\theta_3 = \frac{3-\gamma}{2}\left(\Delta_2\text{sign}(\Upsilon_i)\right)^{\gamma-1}, \quad \theta_4 = \frac{\gamma-1}{2}\left(\Delta_2\text{sign}(\Upsilon_i)\right)^{\gamma-3}$$

Remark 7. The given θ_i, $i = 1, \ldots, 4$ are used to guarantee continuous solutions to φ_ε, φ_Υ and their derivatives $\dot{\varphi}_\varepsilon$, $\dot{\varphi}_\Upsilon$ even though their forms are changed due to the different cases for ε and Υ. Therefore, the switch terms φ_ε and φ_Υ can provide a smooth and continuous output. In addition, the smooth and continuous outputs for φ_ε and φ_Υ avoid the chattering phenomenon when φ_ε and φ_Υ change their forms with respect to ε and Υ. Invoking by the nonsingular terminal sliding mode control method, the singular problem is also avoided. Comparing with the fractional form in φ_ε and φ_Υ, the polynomial cases with cubic forms will not lead to the singular problem when ε and Υ approach the origin.

Theorem 1. *For the rigid satellite attitude system (1) and (2) with input delay and saturation, the tracking error $\tilde{\sigma}$ and $\bar{\omega}$ are ultimately uniformly bounded by utilizing the proposed controller (34) and (39) while the predesigned output constraints for $\tilde{\sigma}$ and ε are maintained. In addition, the convergent performances of $\tilde{\sigma}$ and $\bar{\omega}$ are categorized as follows,*

- *For the case when $|\varepsilon_i| \geq \Delta_1$ and $|\Upsilon_i| \geq \Delta_2$, $\tilde{\sigma}$ and $\bar{\omega}$ can converge to the neighborhood of the origin within a finite time.*

- *For other cases, $\tilde{\sigma}$ and $\bar{\omega}$ can asymptotically converge to the neighborhood of the origin.*

Proof: Define the following Lyapunov function,

$$V_{1m} = V_1 + \frac{1}{2\kappa_1} \tilde{\varrho}^2$$

where $\tilde{\varrho} = \varrho - \hat{\varrho}$. Considering (33)-(35), the time derivative of V_{1m} satisfies,

$$
\begin{aligned}
\dot{V}_{1m} = & - k_1 \sum_{i=1}^{3} \frac{\varepsilon_i^2}{k_b^2 - \varepsilon_i^2} - k_{\varphi_1} \sum_{i=1}^{3} \frac{\varepsilon_i}{k_b^2 - \varepsilon_i^2} \varphi_{\varepsilon_i} \\
& + \varepsilon^T F(\varepsilon) \Phi G \Upsilon + \varepsilon^T F(\varepsilon) \bar{F} \\
& - \varepsilon^T F(\varepsilon) \left(\frac{F(\varepsilon)}{2\epsilon} + \frac{\hat{\varrho} F(\varepsilon) \phi}{2\eta} \right) \varepsilon + \frac{k_{\varrho}}{\kappa_1} \tilde{\varrho} \hat{\varrho} \\
& - \tilde{\varrho} \frac{\sum_{i=1}^{3} \frac{\varepsilon_i^2}{(k_b^2 - \varepsilon_i^2)^2} \phi_i^T \phi_i}{2\eta} + \frac{k_{\varrho}}{\kappa_1} \tilde{\varrho} \left(\hat{\varrho} - \ell_{\varrho} \right)
\end{aligned}
\tag{41}
$$

where $\bar{F} = \Phi G \left(-J^{-1} D \chi / \lambda + J^{-1} D \zeta + \omega_\Delta \right)$. The following equality is valid with reference to Lemma 1,

$$\bar{F}_i = \varrho_i^T \phi_i(\varepsilon_i) + \hbar_i, \ i = 1, 2, 3$$

where $\bar{F}_i$ is the ith element in $\bar{F}$. ϱ_i and ϕ_i are the weight vector and the fuzzy basis function vector, respectively. $\hbar_i$ is the approximation error introduced by the FLS. In addition, it can be found that,

$$
\begin{aligned}
\sum_{i=1}^{3} \frac{\varepsilon_i}{k_b^2 - \varepsilon_i^2} \bar{F}_i \leq & \sum_{i=1}^{3} \frac{\varepsilon_i}{k_b^2 - \varepsilon_i^2} \varrho_i^T \phi_i(\varepsilon_i) + \sum_{i=1}^{3} \frac{|\varepsilon_i|}{k_b^2 - \varepsilon_i^2} |\hbar_i| \\
& \leq \sum_{i=1}^{3} \frac{\frac{\varepsilon_i^2}{(k_b^2 - \varepsilon_i^2)^2} \varrho \phi_i^T \phi_i}{2\eta} + \frac{3\eta}{2} + \sum_{i=1}^{3} \frac{\varepsilon_i^2}{2\epsilon(k_b^2 - \varepsilon_i^2)^2} + \frac{3}{2} \epsilon \hbar^2
\end{aligned}
$$

where $\hbar = \max\{|\hbar_1|, |\hbar_2|, |\hbar_3|\}$.

As for $(k_{\varrho}/\kappa_1) \tilde{\varrho} \hat{\varrho}$ and $(k_{\varrho}/\kappa_1) \tilde{\varrho} \left(\hat{\varrho} - \ell_{\varrho} \right)$, it holds,

$$\frac{k_{\varrho}}{\kappa_1} \tilde{\varrho} \hat{\varrho} = \frac{k_{\varrho}}{\kappa_1} \tilde{\varrho}(\varrho - \tilde{\varrho}) \leq -\frac{3 k_{\varrho} \tilde{\varrho}^2}{4\kappa_1} + \frac{k_{\varrho} \varrho^2}{\kappa_1}$$

$$\frac{k_{\varrho}}{\kappa_1} \tilde{\varrho} \left(\hat{\varrho} - \ell_{\varrho} \right) \leq -\frac{k_{\varrho}}{2\kappa_1} \tilde{\varrho}^2 + \frac{k_{\varrho}}{2\kappa_1} \left(\varrho - \ell_{\varrho} \right)^2$$

Noting that $0 < \gamma < 1$, from [40], it concludes that,

$$\left(\frac{k_{\varrho} \tilde{\varrho}^2}{2\kappa_1} \right)^{\frac{1+\gamma}{2}} - \frac{k_{\varrho} \tilde{\varrho}^2}{2\kappa_1} \leq \frac{1}{4}$$

Therefore, (41) satisfies,

$$
\begin{aligned}
\dot{V}_{1m} \leq & -k_1 \sum_{i=1}^{3} \frac{\varepsilon_i^2}{k_b^2 - \varepsilon_i^2} - k_{\varphi_1} \sum_{i=1}^{3} \frac{\varepsilon_i}{k_b^2 - \varepsilon_i^2} \varphi_{\varepsilon_i} + \varepsilon^T F(\varepsilon) \Phi G \Upsilon \\
& + \frac{3\eta}{2} + \sum_{i=1}^{3} \frac{\varepsilon_i^2}{2\epsilon(k_b^2 - \varepsilon_i^2)^2} + \frac{3}{2}\epsilon\hbar^2 - \sum_{i=1}^{3} \frac{\varepsilon_i^2}{2\epsilon(k_b^2 - \varepsilon_i)^2} \\
& + \sum_{i=1}^{3} \frac{\frac{\varepsilon_i^2}{(k_b^2-\varepsilon_i^2)^2}\varrho\phi_i^T\phi_i}{2\eta} - \sum_{i=1}^{3} \frac{\hat{\varrho}\varepsilon_i^2\phi_i^T\phi_i}{2\eta(k_b^2-\varepsilon_i^2)^2} - \tilde{\varrho}\frac{\sum_{i=1}^{3}\frac{\varepsilon_i^2}{(k_b^2-\varepsilon_i^2)^2}\phi_i^T\phi_i}{2\eta} \\
& - \frac{3k_\varrho\tilde{\varrho}^2}{4\kappa_1} + \frac{k_\varrho\varrho^2}{\kappa_1} - \left(\frac{k_\varrho\tilde{\varrho}^2}{2\kappa_1}\right)^{\frac{1+\gamma}{2}} + \frac{1}{4} + \frac{k_\varrho}{2\kappa_1}\left(\varrho - \ell_\varrho\right)^2 \\
\leq & -k_1 \sum_{i=1}^{3} \frac{\varepsilon_i^2}{k_b^2 - \varepsilon_i^2} - k_{\varphi_1} \sum_{i=1}^{3} \frac{\varepsilon_i}{k_b^2 - \varepsilon_i^2} \varphi_{\varepsilon_i} - \frac{3k_\varrho\tilde{\varrho}^2}{4\kappa_1} \\
& + \varepsilon^T F(\varepsilon) \Phi G \Upsilon - \left(\frac{k_\varrho\tilde{\varrho}^2}{2\kappa_1}\right)^{\frac{1+\gamma}{2}} + \Delta V_{m1}
\end{aligned}
\tag{42}
$$

where $\Delta V_{m1} = 3\eta/2 + 3\epsilon\hbar^2/2 + k_\varrho\varrho^2/\kappa_1 + 1/4 + k_\varrho/(2\kappa_1)\left(\varrho - \ell_\varrho\right)^2$.

Then, constructing V_{2m} as follows,

$$
V_{2m} = V_{1m} + \frac{1}{2}\Upsilon^T\Upsilon + \frac{1}{2\kappa_2}\tilde{E}^T\tilde{E}
$$

By considering (42), the derivative for V_{2m} holds,

$$
\begin{aligned}
\dot{V}_{2m} \leq & -k_1 \sum_{i=1}^{3} \frac{\varepsilon_i^2}{k_b^2 - \varepsilon_i^2} - k_{\varphi_1} \sum_{i=1}^{3} \frac{\varepsilon_i}{k_b^2 - \varepsilon_i^2} \varphi_{\varepsilon_i} \\
& + \Upsilon^T G^T \Phi F(\varepsilon)\varepsilon - \frac{3k_\varrho\tilde{\varrho}^2}{4\kappa_1} - \left(\frac{k_\varrho\tilde{\varrho}^2}{2\kappa_1}\right)^{\frac{1+\gamma}{2}} + \Delta V_{m1} + \frac{1}{\kappa_2}\tilde{E}^T\dot{\tilde{E}} \\
& + \Upsilon^T \left[-J^{-1}\omega^\times J\omega + J^{-1}Dv + J^{-1}D\zeta + J^{-1}(De_s(v) + T_d) - \dot{\omega}_c\right] \\
\leq & -k_1 \sum_{i=1}^{3} \frac{\varepsilon_i^2}{k_b^2 - \varepsilon_i^2} - k_{\varphi_1} \sum_{i=1}^{3} \frac{\varepsilon_i}{k_b^2 - \varepsilon_i^2} \varphi_{\varepsilon_i} - \frac{3k_\varrho\tilde{\varrho}^2}{4\kappa_1} - \left(\frac{k_\varrho\tilde{\varrho}^2}{2\kappa_1}\right)^{\frac{1+\gamma}{2}} + \Delta V_{m1} + \Upsilon^T E \\
& + \Upsilon^T \left(-J^{-1}\omega^\times J\omega + J^{-1}Dv + J^{-1}D\zeta - \dot{\omega}_c\right) \\
& - \frac{1}{\kappa_2}\tilde{E}^T\left[\kappa_2\tanh(\Upsilon/z)\Upsilon - k_E\left(2\hat{E} - \ell_E\right)\right]
\end{aligned}
\tag{43}
$$

where $E = G^T\Phi F(\varepsilon)\varepsilon + J^{-1}(De_s(v) + T_d)$. According to Assumption 1, E is a bounded variable. By retrospecting Lemma 3, it can be found that,

$$
\begin{aligned}
\Upsilon^T E \leq & \sum_{i=1}^{3} |\Upsilon_i|\bar{E}_i \leq \sum_{i=1}^{3} \left(\Upsilon_i\tanh(\Upsilon_i/z)\bar{E}_i + k_z z\bar{E}_i\right) \\
\leq & \Upsilon^T\tanh(\Upsilon/z)\bar{E} + \sum_{i=1}^{3} k_z z\bar{E}_i \\
= & \Upsilon^T\tanh(\Upsilon/z)\bar{E} + \Delta_{\bar{E}}
\end{aligned}
\tag{44}
$$

where z is a positive scalar and $\tanh(\Upsilon/z) = \mathrm{diag}\{[\tanh(\Upsilon_1/z); \tanh(\Upsilon_2/z); \tanh(\Upsilon_3/z)]\}$. $\bar{E}_i$ is the upper bound for the ith element in E and $\bar{E} = [\bar{E}_1; \bar{E}_2; \bar{E}_3]$. Substituting (39) and (44) into (43), it obtains that,

$$
\begin{aligned}
\dot{V}_{2m} \leq &- k_1 \sum_{i=1}^{3} \frac{\varepsilon_i^2}{k_b^2 - \varepsilon_i^2} - k_{\varphi_1} \sum_{i=1}^{3} \frac{\varepsilon_i}{k_b^2 - \varepsilon_i^2} \varphi_{\varepsilon_i} \\
&- \frac{3k_\varrho \tilde{\varrho}^2}{4\kappa_1} - \left(\frac{k_\varrho \tilde{\varrho}^2}{2\kappa_1} \right)^{\frac{1+\gamma}{2}} + \Delta V_{m1} - k_2 \Upsilon^T \Upsilon \\
&- k_{\varphi_2} \Upsilon^T \varphi_\Upsilon + \Delta_{\bar{E}} + \frac{k_E}{\kappa_2} \tilde{E}^T \hat{E} + \frac{k_E}{\kappa_2} \tilde{E}^T \left(\hat{E} - \ell_E \right)
\end{aligned}
\tag{45}
$$

Similarly to the previous deduction, we have,

$$
\begin{aligned}
\frac{k_E}{\kappa_2} \tilde{E}^T \hat{E} &\leq - \frac{3k_E}{4\kappa_2} \sum_{i=1}^{3} \tilde{E}_i^2 + \sum_{i=1}^{3} \frac{k_E}{\kappa_2} \bar{E}_i^2 \\
&= - \frac{3k_E}{4\kappa_2} \tilde{E}^T \tilde{E} + \frac{k_E}{\kappa_2} \bar{E}^T \bar{E}
\end{aligned}
$$

$$
\frac{k_E}{\kappa_2} \tilde{E}^T \left(\hat{E} - \ell_E \right) \leq - \frac{k_E}{2\kappa_2} \tilde{E}^T \tilde{E} + \frac{k_E}{2\kappa_2} \left(\bar{E} - \ell_E \right)^T \left(\bar{E} - \ell_E \right)
$$

$$
\begin{aligned}
- \frac{k_E}{2\kappa_2} \tilde{E}^T \tilde{E} &\leq \sum_{i=1}^{3} - \left(\frac{k_E}{2\kappa_2} \tilde{E}_i^2 \right)^{\frac{1+\gamma}{2}} + \frac{3}{4} \\
&= - \left(\frac{k_E}{2\kappa_2} \tilde{E}^T \tilde{E} \right)^{\frac{1+\gamma}{2}} + \frac{3}{4}
\end{aligned}
$$

Furthermore, (45) can be formulated as,

$$
\begin{aligned}
\dot{V}_{2m} \leq &- k_1 \sum_{i=1}^{3} \frac{\varepsilon_i^2}{k_b^2 - \varepsilon_i^2} - k_{\varphi_1} \sum_{i=1}^{3} \frac{\varepsilon_i}{k_b^2 - \varepsilon_i^2} \varphi_{\varepsilon_i} \\
&- \frac{3k_\varrho \tilde{\varrho}^2}{4\kappa_1} - \left(\frac{k_\varrho \tilde{\varrho}^2}{2\kappa_1} \right)^{\frac{1+\gamma}{2}} - k_2 \Upsilon^T \Upsilon - k_{\varphi_2} \Upsilon^T \varphi_\Upsilon \\
&- \frac{3k_E}{4\kappa_2} \tilde{E}^T \tilde{E} - \left(\frac{k_E}{2\kappa_2} \tilde{E}^T \tilde{E} \right)^{\frac{1+\gamma}{2}} + \Delta V_{m2}
\end{aligned}
\tag{46}
$$

where $\Delta V_{m2} = \Delta V_{m1} + \Delta_{\bar{E}} + (k_E/\kappa_2)\bar{E}^T \bar{E} + 3/4 + (k_E/(2\kappa_2)) \left(\bar{E} - \ell_E \right)^T \left(\bar{E} - \ell_E \right)$.

1) For the case when $|\varepsilon_i| \geq \Delta_1$ and $|\Upsilon_i| \geq \Delta_2$, (46) holds,

$$
\begin{aligned}
\dot{V}_{2m} \leq &- k_1 \sum_{i=1}^{3} \log \frac{k_b^2}{k_b^2 - \varepsilon_i^2} - k_{\varphi_1} \sum_{i=1}^{3} \left(\log \frac{k_b^2}{k_b^2 - \varepsilon_i^2} \right)^{\frac{1+\gamma}{2}} \\
&- \frac{3k_\varrho \tilde{\varrho}^2}{4\kappa_1} - \left(\frac{k_\varrho \tilde{\varrho}^2}{2\kappa_1} \right)^{\frac{1+\gamma}{2}} - k_2 \Upsilon^T \Upsilon - k_{\varphi_2} (\Upsilon^T \Upsilon)^{\frac{1+\gamma}{2}} \\
&- \frac{3k_E}{4\kappa_2} \tilde{E}^T \tilde{E} - \left(\frac{k_E}{2\kappa_2} \tilde{E}^T \tilde{E} \right)^{\frac{1+\gamma}{2}} + \Delta V_{m2} \\
\leq &- k_3 V_{2m} - k_4 V_{2m}^{\frac{1+\gamma}{2}} + \Delta V_{m2}
\end{aligned}
\tag{47}
$$

where $k_3 = \min\left\{2k_1, 2k_2, 3k_\varrho/2, 3k_E/2\right\}$ and $k_4 = \min\left\{2^{\frac{1+\gamma}{2}}k_{\varphi 1}, 2^{\frac{1+\gamma}{2}}k_{\varphi 2}, k_\varrho^{\frac{1+\gamma}{2}}, k_E^{\frac{1+\gamma}{2}}\right\}$.

According to Proposition 1, we note that V_{2m} converges to $V_{2m} \le \frac{\Delta V_{m2}}{(1-c)k_3}$ within a finite time and $0 < c < 1$. Therefore, it indicates that,

$$|\varepsilon_i| \le \sqrt{1 - \exp\left(-\frac{2\Delta V_{m2}}{(1-c)k_3}\right)}, i = 1, 2, 3$$

$$|\tilde\varrho| \le \sqrt{\frac{2\kappa_1 \Delta V_{m2}}{(1-c)k_3}}, \quad \|\Upsilon\| \le \sqrt{\frac{2\Delta V_{m2}}{(1-c)k_3}}, \quad \|\tilde{\tilde{E}}\| \le \sqrt{\frac{2\kappa_2 \Delta V_{m2}}{(1-c)k_3}}$$

In addition, the reaching time T_{reach} for this case is as,

$$T_{reach} \le \frac{2}{ck_3(1-\gamma)}\log\frac{ck_3 V_{2m}^{\frac{1-\gamma}{2}}(0) + k_4}{k_4}$$

2) For the case when $|\varepsilon_i| < \Delta_1$ and $|\Upsilon_i| < \Delta_2$, (46) holds,

$$
\begin{aligned}
\dot V_{2m} \le & -k_1 \sum_{i=1}^{3}\log\frac{k_b^2}{k_b^2 - \varepsilon_i^2} - k_{\varphi 1}\theta_1\sum_{i=1}^{3}\log\frac{k_b^2}{k_b^2 - \varepsilon_i^2} - \frac{3k_\varrho \tilde\varrho^2}{4\kappa_1} \\
& - k_2 \Upsilon^T\Upsilon - k_{\varphi 2}\theta_3\Upsilon^T\Upsilon - \frac{3k_E}{4\kappa_2}\tilde{\tilde{E}}^T\tilde{\tilde{E}} + \Delta V_{m2} \\
\le & -k_5 V_{2m} + \Delta V_{m2}
\end{aligned}
\tag{48}
$$

where $k_5 = \min\left\{2(k_1 + k_{\varphi 1}\theta_1), 2(k_2 + k_{\varphi 2}\theta_3), 3k_\varrho/2, 3k_E/2\right\}$.

According to Gronwall's Inequality, it concludes that,

$$V_{2m} \le \left(V_{2m}(0) - \frac{\Delta V_{m2}}{k_5}\right)\exp(-k_5 t) + \frac{\Delta V_{m2}}{k_5}$$

The boundary sets for tracking errors and other variables are shown as,

$$|\varepsilon_i| \le \sqrt{1 - \exp\left(-2\left(V_{2m}(0) - \frac{\Delta V_{m2}}{k_5}\right)\exp(-k_5 t) - 2\frac{\Delta V_{m2}}{k_5}\right)}, i = 1, 2, 3$$

$$|\tilde\varrho| \le \sqrt{2\kappa_1\left[\left(V_{2m}(0) - \frac{\Delta V_{m2}}{k_5}\right)\exp(-k_5 t) + \frac{\Delta V_{m2}}{k_5}\right]}$$

$$\|\Upsilon\| \le \sqrt{2\left[\left(V_{2m}(0) - \frac{\Delta V_{m2}}{k_5}\right)\exp(-k_5 t) + \frac{\Delta V_{m2}}{k_5}\right]}$$

$$\|\tilde{\tilde{E}}\| \le \sqrt{2\kappa_2\left[\left(V_{2m}(0) - \frac{\Delta V_{m2}}{k_5}\right)\exp(-k_5 t) + \frac{\Delta V_{m2}}{k_5}\right]}$$

3) For the case when $|\varepsilon_i| \ge \Delta_1$ and $|\Upsilon_i| < \Delta_2$, (46) holds,

$$
\begin{aligned}
\dot V_{2m} \le & -k_1\sum_{i=1}^{3}\log\frac{k_b^2}{k_b^2 - \varepsilon_i^2} - k_{\varphi 1}\sum_{i=1}^{3}\left(\log\frac{k_b^2}{k_b^2 - \varepsilon_i^2}\right)^{\frac{1+\gamma}{2}} \\
& - \frac{3k_\varrho\tilde\varrho^2}{4\kappa_1} - \left(\frac{k_\varrho\tilde\varrho^2}{2\kappa_1}\right)^{\frac{1+\gamma}{2}} - k_2\Upsilon^T\Upsilon
\end{aligned}
$$

$$- k_{\varphi 2}\theta_3\Upsilon^T\Upsilon - \frac{3k_E}{4\kappa_2}\tilde{\tilde{E}}^T\tilde{\tilde{E}} + \Delta V_{m2}$$

$$\leq - k_6 V_{2m} + \Delta V_{m2} \tag{49}$$

where $k_6 = \min\{2k_1, 2(k_2 + k_{\varphi 2}\theta_3), 3k_\varrho/2, 3k_E/2\}$. Similarly, the variables hold the same forms of the tolerance boundary in Case 2 with different gain parameters.

4) For the case when $|\varepsilon_i| < \Delta_1$ and $|\Upsilon_i| \geq \Delta_2$, (46) has the similar solution in (49).

$$\dot{V}_{2m} \leq - k_1 \sum_{i=1}^{3} \log \frac{k_b^2}{k_b^2 - \varepsilon_i^2} - k_{\varphi 1}\theta_1 \sum_{i=1}^{3} \log \frac{k_b^2}{k_b^2 - \varepsilon_i^2} - \frac{3k_\varrho \tilde{\varrho}^2}{4\kappa_1}$$

$$- k_2 \Upsilon^T\Upsilon - k_{\varphi 2}\left(\Upsilon^T\Upsilon\right)^{\frac{1+\gamma}{2}} - \frac{3k_E}{4\kappa_2}\tilde{\tilde{E}}^T\tilde{\tilde{E}} + \Delta V_{m2}$$

$$\leq - k_7 V_{2m} + \Delta V_{m2} \tag{50}$$

where $k_7 = \min\{2(k_1 + k_{\varphi 1}\theta_1), 2k_2, 3k_\varrho/2, 3k_E/2\}$. In addition, the tolerance boundaries for the variables hold the same forms like Case 2 with different gain parameters.

According to the previous four cases, the tracking error $\tilde{\sigma}$ and $\bar{\omega}$ are forced to converge to the neighborhood of the origin. The main difference between these cases is that the finite time convergence can be guaranteed only in Case 1 while the asymptotical convergence is maintained for Case 2-4.

<div align="right">□</div>

Remark 8. Although (47)-(50) provide an ultimately uniformly bounded result, the solutions set for ε_i, $\tilde{\varrho}$, Υ and $\tilde{\tilde{E}}$ can be small enough by selecting proper control parameters with respect to different cases of Δ_1 and Δ_2. In other words, ε_i, $\tilde{\varrho}$, Υ and $\tilde{\tilde{E}}$ can be forced to converge to an arbitrarily small neighborhood of the origin and the finite time convergence can be ensured for a certain case. In order to accelerate the convergent process, Δ_1 and Δ_2 can be chosen small such that the occurrence possibility for Case 1 can be increased. However, there exists a tradeoff for the selections of Δ_1 and Δ_2 when considering the singularity problem. Therefore, the proper selections of Δ_1 and Δ_2 are based on the designer's demands on the time response and the output performance.

Remark 9. In this control strategy, a novel BLF-based PPC control framework is constructed. In many existing BLF researches, the boundary constraint is usually set for the tracking error. As for the wildly used PPC approaches, they focus on the constraint on the tracking error while the constraint for the unconstrained variable is not considered. For this research, the constrained variable in BLF is transformed into the unconstrained variable $\varepsilon(t)$ produced by the PPC method. Therefore, the constraints for both the tracking error $\tilde{\sigma}(t)$ and the transformed error $\varepsilon(t)$ are considered in the novel BLF-based PPC control framework.

Remark 10. For many existing BLF methods, they may only provide the asymptotical result for the proposed controller design. By designing the switch terms φ_ε and φ_Υ in the virtual and actual controller, the finite time convergent property for the proposed method can be guaranteed for a certain case. In addition, due to the implement of φ_ε and φ_Υ, the singularity problem in [42, 43] can be avoided when φ_ε and φ_Υ approaches the origin.

5. Simulation

In order to exemplify the effectiveness of the proposed control strategy, some simulation results are given in this section. A classical adaptive backstepping controller in [44] is also considered. The aims of the simulation results involve the demonstrations of the impact caused by time delay and input saturation under the constraint for the attitude tracking error. During the simulation, the inertial matrix is chosen as $J = [20, 1.2, 0.9; 1.2, 17, 1.4; 0.9, 1.4, 15]kg \cdot m^2$ and the desired attitude σ_d is set as $\sigma_d = [0; 0; 0]$ while the initial attitude states for σ and ω are selected as $\sigma(0) = [-0.2; 0.3; -0.3]$ and $\omega(0) = [0; 0; 0]rad/s$ respectively. The control allocation matrix D is $D = I_3$. The maximum control torque provided by each actuator is $u_{\max} = 1Nm$. The external disturbance is assumed as $T_d = 0.01 \times [-3\sin(0.03t); \cos(0.05t); 2\sin(0.02t)]Nm$. The time delay τ is set as $\tau = 0.01s$.

The parameters of the proposed control approach are given in Table. 1. As for the parameters in [44], they are chosen on the basis of trial and error time response such that the controller performance in [44] has the nearly identical

Table 1
Parameters for the proposed control strategy

Module	Parameters
PPC-BLF	$\rho(0) = 0.5$, $\rho_\infty = 0.01$, $l = 3$, $t_f = 30s$, $\mathcal{G}_{i1} = 5$, $\mathcal{G}_{i2} = 2$, $\mathcal{G}_{i3} = 3$, $\mathcal{G}_{i4} = 5$, $\mathcal{G}_{i5} = 3$, $\mathcal{G}_{i6} = 2$, $\varsigma_{i1} = 0.1$, $\varsigma_{i2} = 0.2$, $i = 1, 2, 3$, $k_b = 1$
Virtual Controller	$k_1 = 0.2$, $k_{\varphi 1} = 0.01$, $\epsilon = 10$, $\eta = 1$, $\gamma = 0.8$, $\ell_\varrho = 0.01$, $\kappa_1 = 0.5$, $k_\varrho = 5$, $\Delta_1 = 0.15$
Controller	$k_2 = 0.8$, $z = 0.01$, $k_{\varphi 2} = 0.01$, $\kappa_2 = 5$, $k_E = 0.05$, $\ell_E = [1; 1; 1]$, $\Delta_2 = 0.05$
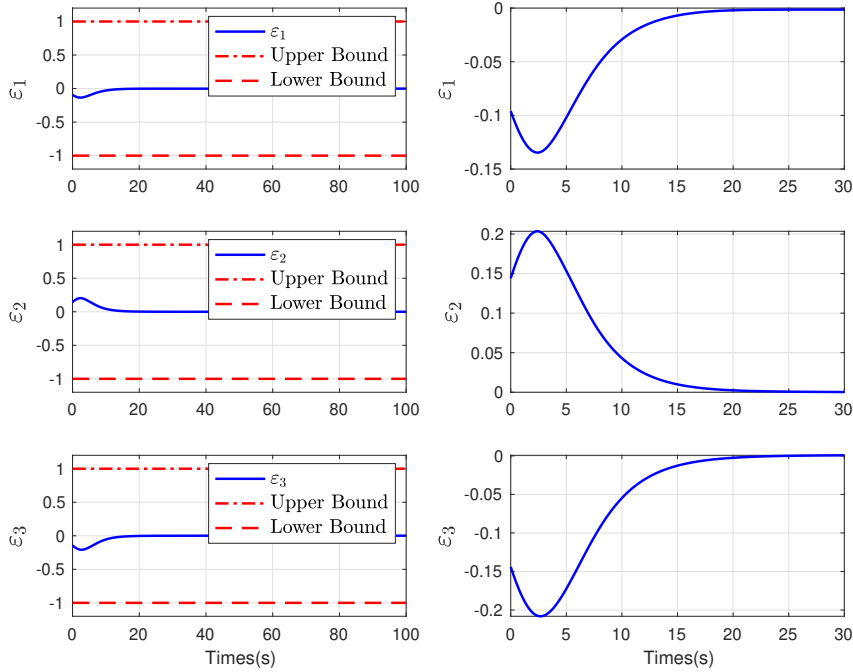
Figure 2: The output of the transformed error ε

time responses of the proposed control approach in this paper. The time response of the transformed error ε is depicted in Fig. 2. It shows that by integrating the criteria of the BLF, the given control strategy can guarantee the variance for the transformed error ε provided by the PPC. Even more, there is no overshoot for the time response of ε during the stabilization process. As a result, this also ensures the non-overshoot time responses of the attitude tracking error $\tilde{\sigma}$ and the response of $\tilde{\sigma}$ is forced to converge to the origin unilaterally along the given PPC boundary. In addition, this statement is validated by Fig. 3. The upper bound for the attitude tracking error $\tilde{\sigma}$ is represented as PUB while the lower bound is denoted as PLB. From Fig. 3, it can be seen that the attitude tracking error can converge to the origin swiftly and the performance constraint marked with red lines is kept from the beginning. Apart from this, the time performance of the control strategy in [44] which is denoted as M2 is revealed with the black dashed line. It shows that the time response of M2 is free from the overshoot as well and demonstrates comparable robustness with respect to the external disturbance. However, the system response of [44] surpasses the boundary constraint and it takes more time to stabilize the tracking error when compared to the proposed control strategy in this research. The time response of ω is depicted in Fig. 4. Although the peak of ω for the proposed method is larger than the one of M2, it can be viewed as a concede for the swift time response. In addition, the larger ω also ensures the prescribed output constraint for $\tilde{\sigma}$.

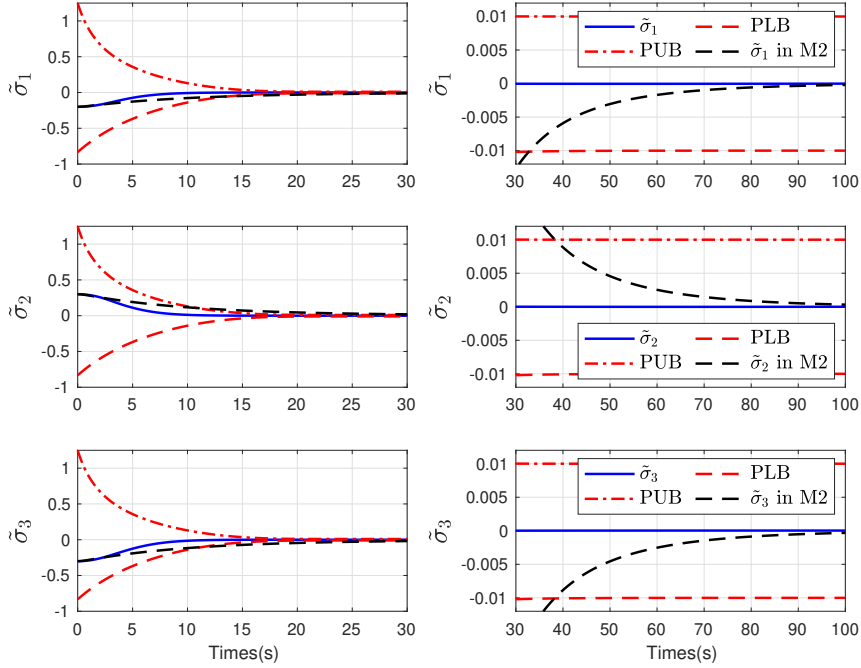The control inputs of the proposed method and the approach in [44] are illustrated in Fig. 5. For the normal

Figure 3: The time response of $\tilde{\sigma}$

controller in [44], it can be seen from [44] that the input delay leads to the chattering phenomenon. This phenomenon degrades the control performance during the attitude tracking process. On the other hand, by taking the input delay into consideration, the proposed method avoids the chattering phenomenon. Due to the implement of the auxiliary system, the control input of the system is continuous as shown in Fig. 6 while the right side of Fig. 6 indicates that the control saturation occurs during this time interval whereas the control signal is continuous before and after the occurrence of the input saturation. As for the attitude σ, the trajectory of σ is given in Fig. 7 where its initial value is marked with red dot. It shows that σ can converge to the origin marked with blue color smoothly.

6. Conclusion

In this paper, the robust output constraint control strategy is proposed along with the input saturation and input delay. The BLF and the PPC methods are implemented such that the proposed control approach can constrain not only the attitude tracking error but also the transformed error generated by the PPC method. The input delay is addressed by the Pade approximation. On account of the auxiliary dynamic system, the impact caused by input saturation is offset. The proposed auxiliary system provides a simpler and reliable way to investigate the controller design compared to the mean value-based method and the Nussbaum function approach. In addition, the switching terms in the controller can guarantee a continuous control input and the stabilization for the tracking error. The future work will focus on the event-triggered methodology design on the basis of the BLF-PPC approach.

Declaration of Competing Interest

There is no conflict of interest in this paper.

Acknowledgement
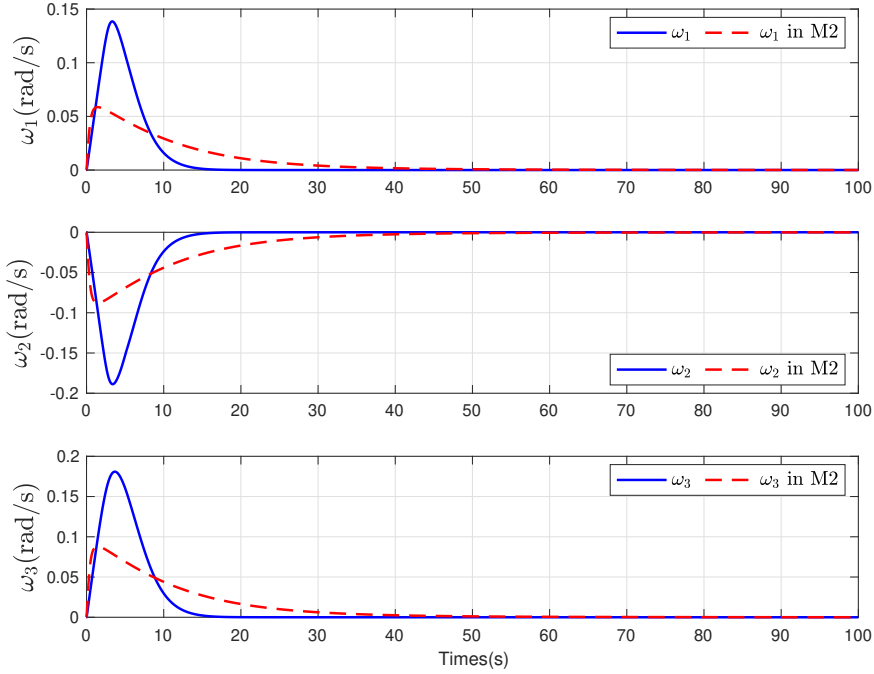
Figure 4: The time response of ω

Appendix

This appendix is focused on verifying the smoothness of φ_ϵ and φ_Υ in (24) and (39) when the cases are changed. Firstly, for $\varphi_{\varepsilon_i}(\varepsilon_i)$, two main scenarios are considered, namely, ε_i approaching Δ_1 and $-\Delta_1$. When $\varepsilon_i = \Delta_1$, we have,

$$\varphi_{\varepsilon_i}(\varepsilon_i) = \Delta_1^\gamma \left(k_b^2 - \Delta_1^2\right)^{\frac{1-\gamma}{2}}$$

$$\dot{\varphi}_{\varepsilon_i}(\varepsilon_i)|_{\varepsilon_i = \Delta_1} = \gamma \varepsilon_i^{\gamma-1} \left(k_b^2 - \varepsilon_i^2\right)^{\frac{1-\gamma}{2}} - \frac{1-\gamma}{2} \varepsilon_i^\gamma \left(k_b^2 - \varepsilon_i^2\right)^{-\frac{1+\gamma}{2}} \times 2\varepsilon_i$$

$$= \gamma \Delta_1^{\gamma-1} \left(k_b^2 - \Delta_1^2\right)^{\frac{1-\gamma}{2}} - (1-\gamma) \Delta_1^{\gamma+1} \left(k_b^2 - \Delta_1^2\right)^{-\frac{1+\gamma}{2}}$$

When $\varepsilon_i < \Delta_1$ and ε_i approaches Δ_1, it can obtain that,

$$\lim_{\varepsilon_i \to \Delta_1} \varphi_{\varepsilon_i}(\varepsilon_i) = \theta_1 \Delta_1 + \theta_2 \Delta_1^3 = \Delta_1^\gamma \left(k_b^2 - \Delta_1^2\right)^{\frac{1-\gamma}{2}}$$

$$\lim_{\varepsilon_i \to \Delta_1} \dot{\varphi}_{\varepsilon_i}(\varepsilon_i) = \Delta_1^{\gamma-1} \left(k_b^2 - \Delta_1^2\right)^{\frac{1-\gamma}{2}} - \frac{1}{2} (\gamma - 1) \Delta_1^{\gamma-1} \left[\left(k_b^2 - \Delta_1\right)^{\frac{1-\gamma}{2}} + \Delta_1^2 \left(k_b^2 - \Delta_1^2\right)^{-\frac{1+\gamma}{2}}\right]$$

$$+ \frac{3}{2} (\gamma - 1) \Delta_1^{\gamma-1} \left[\left(k_b^2 - \Delta_1\right)^{\frac{1-\gamma}{2}} + \Delta_1^2 \left(k_b^2 - \Delta_1^2\right)^{-\frac{1+\gamma}{2}}\right]$$

$$= \gamma \Delta_1^{\gamma-1} \left(k_b^2 - \Delta_1^2\right)^{\frac{1-\gamma}{2}} - (1-\gamma) \Delta_1^{\gamma+1} \left(k_b^2 - \Delta_1^2\right)^{-\frac{1+\gamma}{2}}$$

Therefore, the smoothness of $\varphi_{\varepsilon_i}(\varepsilon_i)$ is guaranteed when ε_i approaches Δ_1 and this result can be applied to the case when ε_i approaches $-\Delta_1$.

Similar to the above deduction, the smoothness of $\varphi_{\Upsilon_i}(\Upsilon_i)$ is analyzed when $\varphi_{\Upsilon_i}(\Upsilon_i)$ approaches Δ_2 and $-\Delta_2$.
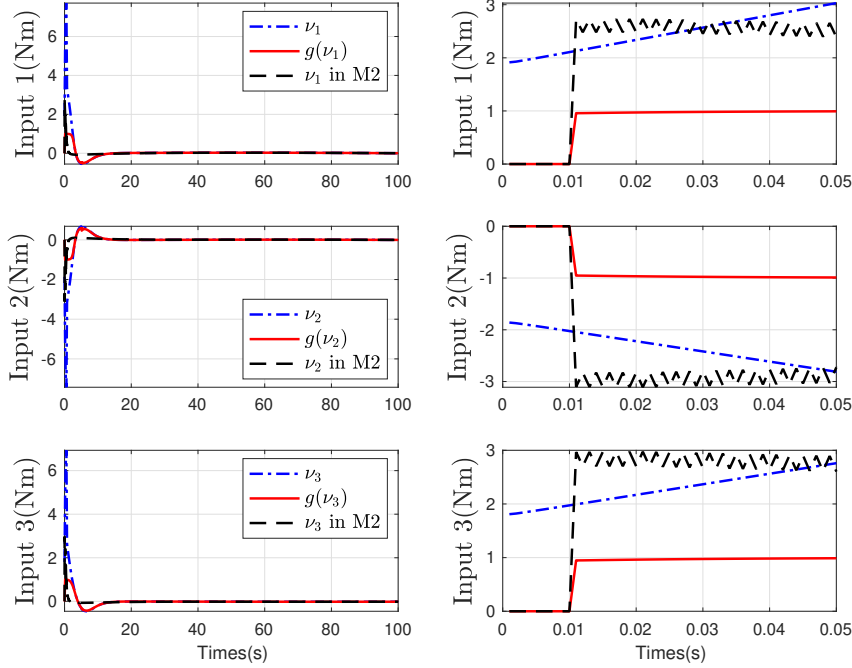
Figure 5: The time response of the control input

When $\Upsilon_i = \Delta_2$, it has that $\varphi_{\Upsilon i}(\Upsilon_i) = \Delta_2^\gamma$ and $\dot{\varphi}_{\Upsilon i}(\Upsilon_i) = \gamma \Delta_2^{\gamma-1}$. When $\Upsilon_i < \Delta_2$ and Υ_i approaches Δ_2, we can have,

$$\lim_{\Upsilon_i \to \Delta_2} \varphi_{\Upsilon i}(\Upsilon_i) = \theta_3 \Delta_2 + \theta_4 \Delta_2^3 = \Delta_2^\gamma$$

$$\lim_{\Upsilon_i \to \Delta_2} \dot{\varphi}_{\Upsilon i}(\Upsilon_i) = \theta_3 + 3\theta_4 \Upsilon_i^2 = \gamma \Delta_2^{\gamma-1}$$

As a result, the smoothness is guaranteed when the cases are switched with respect to Υ_i.

References

[1] L. Sun, Z. Zheng, Disturbance observer-based robust saturated control for spacecraft proximity maneuvers, IEEE Transactions on Control Systems Technology 26 (2) (2018) 684–692.

[2] H. Gui, A. H. J. d. Ruiter, Adaptive fault-tolerant spacecraft pose tracking with control allocation, IEEE Transactions on Control Systems Technology 27 (2) (2019) 479–494.

[3] F. Wang, Y. Miao, C. Li, I. Hwang, Attitude control of rigid spacecraft with predefined-time stability, Journal of the Franklin Institute 357 (7) (2020) 4212–4221.

[4] X. Zhang, Q. Zong, L. Dou, B. Tian, W. Liu, Finite-time attitude maneuvering and vibration suppression of flexible spacecraft, Journal of the Franklin Institute 357 (16) (2020) 11604–11628.

[5] M. Qian, Y. Shi, Z. Gao, X. Zhang, Integrated fault tolerant tracking control for rigid spacecraft using fractional order sliding mode technique, Journal of the Franklin Institute 357 (15) (2020) 10557–10583.

[6] J. Zhang, Z. Wang, X. Zhao, Y. Wang, N. Xu, Prescribed-time observers of lpv systems: A linear matrix inequality approach, Applied Mathematics and Computation 398 (2021) 125982.

[7] W. Sui, G. Duan, M. Hou, M. Zhang, Distributed fixed-time attitude coordinated tracking for multiple rigid spacecraft via a novel integral sliding mode approach, Journal of the Franklin Institute 357 (14) (2020) 9399–9422.

[8] J. Zhang, F. Zhu, H. R. Karimi, F. Wang, Observer-based sliding mode control for T–S fuzzy descriptor systems with time delay, IEEE Transactions on Fuzzy Systems 27 (10) (2019) 2009–2023.

[9] Y. Jinpeng, S. Peng, C. Xinkai, C. Guozeng, Finite-time command filtered adaptive control for nonlinear systems via immersion and invariance, SCIENCE CHINA Information Sciences (1674-733X).

[10] G. Cui, W. Yang, J. Yu, Z. Li, C. Tao, Fixed-time prescribed performance adaptive trajectory tracking control for a QUAV, IEEE Transactions on Circuits and Systems II: Express Briefs (2021) 1–1.
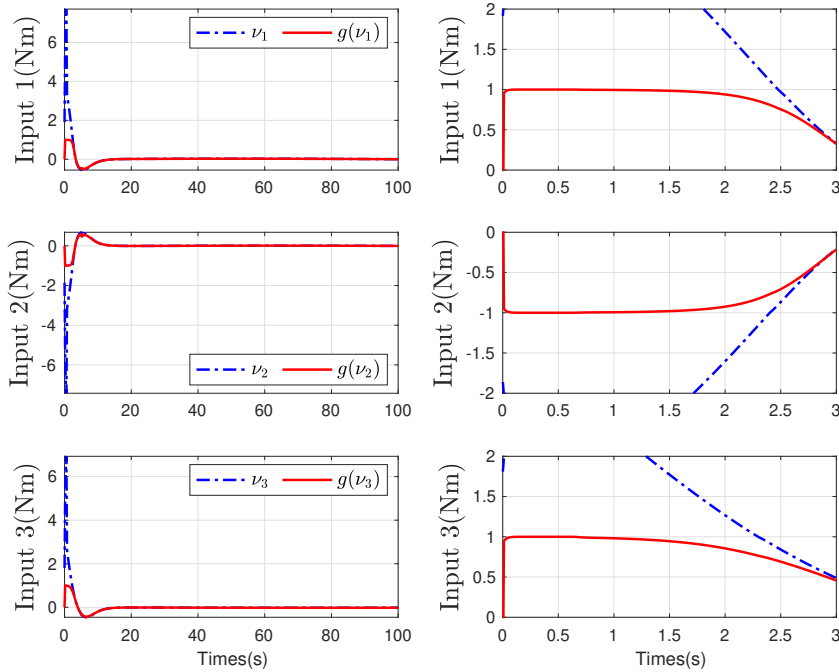
Figure 6: The time response of the control input with saturation

[11] C. Gao, X. Liu, Y. Yang, X. Liu, P. Li, Event-triggered finite-time adaptive neural control for nonlinear non-strict-feedback time-delay systems with disturbances, Information Sciences 536 (2020) 1–24.

[12] G. Cui, W. Yang, J. Yu, Neural network-based finite-time adaptive tracking control of nonstrict-feedback nonlinear systems with actuator failures, Information Sciences 545 (2021) 298–311.

[13] C. Liu, X. Liu, H. Wang, Y. Zhou, S. Lu, Finite-time adaptive tracking control for unknown nonlinear systems with a novel barrier lyapunov function, Information Sciences 528 (2020) 231–245.

[14] Y. Liu, Q. Zhu, N. Zhao, L. Wang, Fuzzy approximation-based adaptive finite-time control for nonstrict feedback nonlinear systems with state constraints, Information Sciences 548 (2021) 101–117.

[15] K. Lu, Y. Xia, Adaptive attitude tracking control for rigid spacecraft with finite-time convergence, Automatica 49 (12) (2013) 3591–3599.

[16] H. Min, S. Xu, X. Yu, S. Fei, G. Cui, Adaptive tracking control for stochastic nonlinear systems with full-state constraints and unknown covariance noise, Applied Mathematics and Computation 385 (2020) 125397.

[17] M. He, T. Rong, J. Li, C. He, Adaptive dynamic surface full state constraints control for stochastic markov jump systems based on event-triggered strategy, Applied Mathematics and Computation 392 (2021) 125563.

[18] Y. Lin, G. Zhuang, W. Sun, J. Zhao, Y. Chu, Resilient $h\infty$ dynamic output feedback controller design for usjss with time-varying delays, Applied Mathematics and Computation 395 (2021) 125875.

[19] H. Li, L. Wang, H. Du, A. Boulkroune, Adaptive fuzzy backstepping tracking control for strict-feedback systems with input delay, IEEE Transactions on Fuzzy Systems 25 (3) (2017) 642–652.

[20] D. Li, Y. Liu, S. Tong, C. L. P. Chen, D. Li, Neural networks-based adaptive control for nonlinear state constrained systems with input delay, IEEE Transactions on Cybernetics 49 (4) (2019) 1249–1258.

[21] Q. Hu, X. Shao, L. Guo, Adaptive fault-tolerant attitude tracking control of spacecraft with prescribed performance, IEEE/ASME Transactions on Mechatronics 23 (1) (2018) 331–341.

[22] X. Shao, Q. Hu, Y. Shi, B. Jiang, Fault-tolerant prescribed performance attitude tracking control for spacecraft under input saturation, IEEE Transactions on Control Systems Technology 28 (2) (2020) 574–582.

[23] M. Zou, J. Yu, Y. Ma, L. Zhao, C. Lin, Command filtering-based adaptive fuzzy control for permanent magnet synchronous motors with full-state constraints, Information Sciences 518 (2020) 1–12.

[24] J. Yu, L. Zhao, H. Yu, C. Lin, Barrier lyapunov functions-based command filtered output feedback control for full-state constrained nonlinear systems, Automatica 105 (2019) 71–79.

[25] H. Wang, B. Chen, X. Liu, K. Liu, C. Lin, Adaptive neural tracking control for stochastic nonlinear strict-feedback systems with unknown input saturation, Information Sciences 269 (2014) 300–315.

[26] Q. Li, J. Yuan, B. Zhang, Extended state observer based output control for spacecraft rendezvous and docking with actuator saturation, ISA Transactions 88 (2019) 37–49.
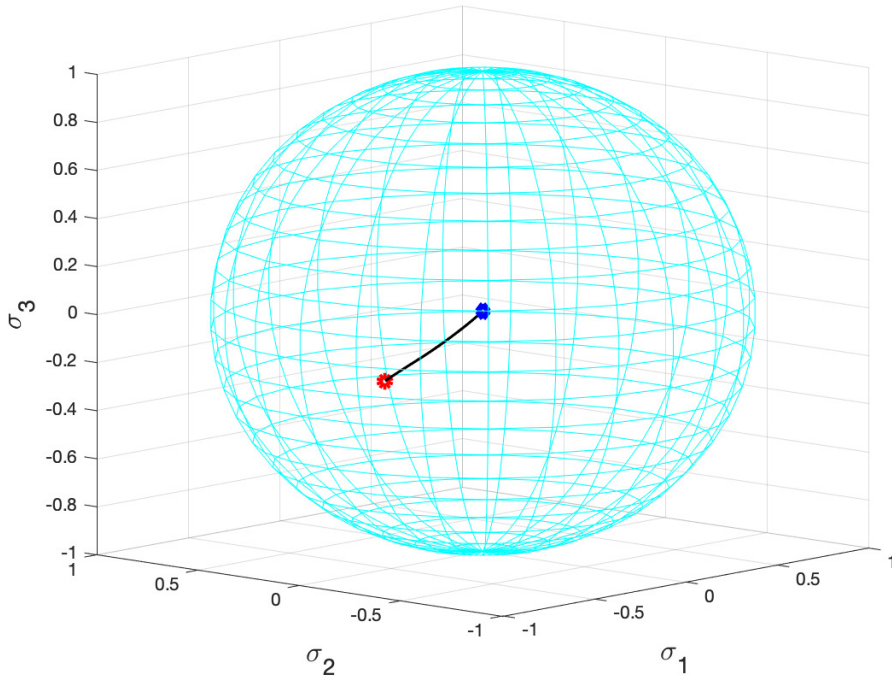
Figure 7: The time response of σ

[27] Z. Zheng, Y. Huang, L. Xie, B. Zhu, Adaptive trajectory tracking control of a fully actuated surface vessel with asymmetrically constrained input and output, IEEE Transactions on Control Systems Technology 26 (5) (2018) 1851–1859.

[28] Y. Li, S. Tong, T. Li, Composite adaptive fuzzy output feedback control design for uncertain nonlinear strict-feedback systems with input saturation, IEEE Transactions on Cybernetics 45 (10) (2015) 2299–2308.

[29] X. Wang, A. Saberi, A. A. Stoorvogel, Stabilization of linear system with input saturation and unknown constant delays, Automatica 49 (12) (2013) 3632–3640.

[30] B. Zhou, H. Gao, Z. Lin, G.-R. Duan, Stabilization of linear systems with distributed input delay and input saturation, Automatica 48 (5) (2012) 712–724.

[31] B. Huo, Y. Xia, L. Yin, M. Fu, Fuzzy adaptive fault-tolerant output feedback attitude-tracking control of rigid spacecraft, IEEE Transactions on Systems, Man, and Cybernetics: Systems 47 (8) (2017) 1898–1908.

[32] S. Shi, Z. Fei, P. Shi, C. K. Ahn, Asynchronous filtering for discrete-time switched T–S fuzzy systems, IEEE Transactions on Fuzzy Systems 28 (8) (2020) 1531–1541.

[33] G. Cui, J. Yu, P. Shi, Observer-based finite-time adaptive fuzzy control with prescribed performance for nonstrict-feedback nonlinear systems, IEEE Transactions on Fuzzy Systems (2020) 1–1.

[34] Z. Liu, H. R. Karimi, J. Yu, Passivity-based robust sliding mode synthesis for uncertain delayed stochastic systems via state observer, Automatica 111 (2020) 108596.

[35] M. A. Khanesar, O. Kaynak, S. Yin, H. Gao, Adaptive indirect fuzzy sliding mode controller for networked control systems subject to time-varying network-induced time delay, IEEE Transactions on Fuzzy Systems 23 (1) (2015) 205–214.

[36] A. Levant, Higher-order sliding modes, differentiation and output-feedback control, International Journal of Control 76 (9-10) (2003) 924–941.

[37] B. Cui, Y. Xia, K. Liu, G. Shen, Finite-time tracking control for a class of uncertain strict-feedback nonlinear systems with state constraints: A smooth control approach, IEEE Transactions on Neural Networks and Learning Systems 31 (11) (2020) 4920–4932.

[38] Y.-X. Li, Finite time command filtered adaptive fault tolerant control for a class of uncertain nonlinear systems, Automatica 106 (2019) 117–123.

[39] F. Wang, B. Chen, C. Lin, J. Zhang, X. Meng, Adaptive neural network finite-time output feedback control of quantized nonlinear systems, IEEE Transactions on Cybernetics 48 (6) (2018) 1839–1848.

[40] J. Yu, L. Zhao, H. Yu, C. Lin, W. Dong, Fuzzy finite-time command filtered control of nonlinear systems with input saturation, IEEE Transactions on Cybernetics 48 (8) (2018) 2378–2387.

[41] Q. Chen, L. Shi, J. Na, X. Ren, Y. Nan, Adaptive echo state network control for a class of pure-feedback systems with input and output constraints, Neurocomputing 275 (2018) 1370–1382.

[42] J. Yu, P. Shi, J. Liu, C. Lin, Neuroadaptive finite-time control for nonlinear mimo systems with input constraint, IEEE transactions on Cybernetics PP.

[43] Z. Liu, J. Yu, Non-fragile observer-based adaptive control of uncertain nonlinear stochastic markovian jump systems via sliding mode technique, Nonlinear Analysis-Hybrid Systems 38 (2020) 100931.

[44] Q. Hu, B. Li, X. Huo, Z. Shi, Spacecraft attitude tracking control under actuator magnitude deviation and misalignment, Aerospace Science and Technology 28 (1) (2013) 266–280.